

# Numerical study of mode-locked semiconductor optical amplifier fiber ring laser

FEI WANG<sup>a,b</sup>, GUANGQIONG XIA<sup>a</sup>, ZHENGMAO WU<sup>a,\*</sup>

<sup>a</sup>*School of Physics, Southwest University, Chongqing 400715, China*

<sup>b</sup>*School of Science, Chongqing Institute of Technology, Chongqing 400050, China*

---

Based on self-reproduction theory, harmonic and rational harmonic mode-locked semiconductor optical amplifier (SOA) fiber ring lasers have been numerically investigated, respectively. Harmonic mode locking makes a target of obtaining ultra-short pulse. While in rational harmonic mode locking, it is urgently needed to solve that pulse amplitude becomes uneven with the increase of the order of rational harmonic. As a result, these two cases result in the different work conditions. After obtaining the optimal work condition, the effects of the system parameters on the characteristics of harmonic mode-locked pulse and the quality of pulse-amplitude equalization in rational harmonic mode locking have been investigated.

(Received January 18, 2006; accepted May 18, 2006)

*Keywords:* Fiber laser, Harmonic mode locking, Rational harmonic mode locking, Semiconductor optical amplifier (SOA), Cross-gain modulation

---

## 1. Introduction

Optical signal sources that are capable of generating wavelength tunable ultra-short pulse train with high quality and high repetition rates play an important role in the optical networks that may combine wavelength division multiplexing (WDM) and optical time domain multiplexing (OTDM) transmission techniques. On the one hand, actively mode-locked fiber laser capable of generating ultra-short transform-limited optical pulse train has attracted people's especial research interests [1-4]. However, the pulse output from the actively mode-locked fiber laser is inherently unstable because of the fluctuations of polarization state and cavity-length drift caused by mechanical vibration and thermal fluctuations. Semiconductor optical amplifier (SOA), with such advantages as rapid response, high stability, polarization independence etc, has been used in fiber laser. SOA acted as the gain medium compared with erbium-doped fiber amplifier (EDFA) can suppress pulse-amplitude fluctuation and supermode noise [5, 6], and can also act as a mode locker [7,8]. Recently, a novel model of backward-optical-injection harmonic mode-locked fiber ring laser consisting of two SOAs has been proposed and preliminary experimental and theoretical results have been reported [9,10]. On the other hand, a high repetition rate pulse train can be obtained by applying rf drive frequency slightly deviated from the multiple of the fundamental

cavity frequency. However, with the increase of the order of rational harmonic, the mode-locked pulse amplitude becomes uneven, which give rise to problems in a real communication environment. At present, many methods have been proposed to realize pulse-amplitude equalization [11-14]. However, the complex configuration results in system stability decline and cost increase. Fortunately, rational harmonic mode-locked (RHML) SOA fiber ring lasers can directly generate an output pulse train with a small amplitude ripple by adjusting system parameters. As mentioned above, harmonic mode locking makes a target of obtaining ultra-short pulse, whereas rational harmonic mode locking focuses on pulse-amplitude equalization, which results in the different work conditions of both. In this paper, mode-locked SOA fiber ring lasers have been numerically investigated, and some new conclusions have been given.

## 2. Theoretical model

The schematic diagram of mode-locked SOA fiber ring laser [9,10] is shown in Fig. 1. A modulated optical signal provided by a gain-switch distributed-feedback laser diode (DFBLD) passes through an optical circulator, then injects into the first SOA (called as the modulation SOA), the second SOA (called as the gain SOA) functions as gain compensator provides the necessary gain, and two Faraday

optical isolators ensure a unidirectional propagation. In order to obtain harmonic mode-locked pulse, the frequency ( $f_m$ ) of the modulated optical signal should be nearly integer times of the cavity fundamental frequency ( $f_c$ ), that is to say,  $f_m = n f_c$  ( $n$  is a positive integer). So the  $n$ th-order harmonic mode-locked pulse series, whose repetition rate ( $f_r$ ) is the same as the modulating frequency, is output from optical coupler with a power-splitting ratio of 95:5. if  $f_m$  satisfies the expression  $f_m = (n + k/p) f_c$  ( $k < p$ , and  $k/p$  is proper fraction), a RHML pulse series whose repetition rate ( $f_r$ ) is  $p f_m$  will be obtained.

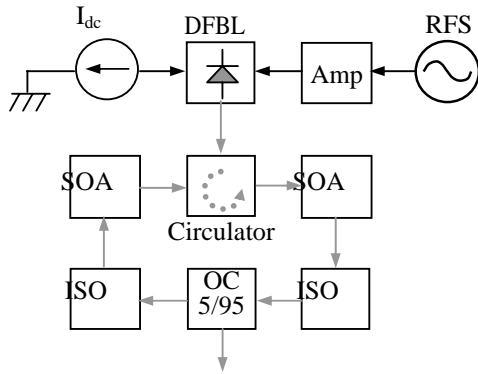


Fig. 1. Schematic diagram of mode-locked SOA fiber ring laser, where RFS, rf synthesizer; Amp, power amplifier; ISO, optical isolator; Circulator, optical circulator; OC, optical coupler.

In this paper, a traveling-wave rate-equation model [9, 10] is adopted to simulate the mode-locked pulse shape and the counterclockwise parts of the traveling-wave equations are neglected because of the existence of the Faraday optical isolators. In general, when the pulse train passes through a SOA, the carrier density in the cavity will vary with both time and space. In order to describe accurately the propagation characteristics of pulse in SOA, the SOA is spliced into 20 sections in the simulation. The gain depletion effects induced by the mode-locked pulse and the backward-optical-injection signal in the modulation SOA, and the asymmetric gain of the SOA have been taken into consideration. The differential rate equations for the carrier density in the  $j$ th section of the modulation SOA, and the propagation equations that describe the time-varied powers of the mode-locked signal pulse and the modulation signal in the modulation SOA, can be written as

$$\frac{\partial N_j(z, T)}{\partial T} = \frac{I}{qV} - \frac{N_j(z, T)}{\tau_c} - \left[ \frac{\Gamma g_{m,j}(z, T)}{h\nu_m A_{cross}} \overline{P_{m,j}} + \frac{\Gamma g_{l,j}(z, T)}{h\nu_l A_{cross}} \overline{P_{l,j}} \right] \quad (1)$$

$$\frac{\partial \overline{P_{m,j}}(z, T)}{\partial z} = -[\Gamma g_{m,j}(z, T) - \alpha_{int}] \overline{P_{m,j}}(z, T) \quad (2)$$

$$\frac{\partial \overline{P_{l,j}}(z, T)}{\partial z} = [\Gamma g_{l,j}(z, T) - \alpha_{int}] \overline{P_{l,j}}(z, T) \quad (3)$$

where the subscripts  $m$  and  $l$  denote the parameters of modulated and mode-locked signal, respectively,  $N_j$  is the carrier density in the  $j$ th section of the SOA,  $T (= t - z / v_g$ , where  $v_g$  is the group velocity in the SOA) represents the time in a reference frame moving along with the pulse,  $I$  is the injection current,  $V$  is the volume of the SOA,  $q$  denotes the electron charge,  $h\nu$  is the photon energy,  $\Gamma$  is the confinement factor,  $A_{cross}$  represents the cross-sectional area of the active layer in the SOA. The carrier lifetime is defined as  $\tau_c^{-1} = A + BN + CN^2$ , where  $A$ ,  $B$  and  $C$  represent the non-radiative recombination, the spontaneous emission and the Auger recombination process, respectively,  $\alpha_{int}$  is the internal loss of the SOA,  $\overline{P_{m,j}}$  and  $\overline{P_{l,j}}$  are the average powers of modulation and mode-locked signal in the  $j$ th section of the SOA, respectively, and can be expressed by

$$\overline{P_{m,j}} = \frac{1}{-\Delta L} \int_0^{-\Delta L} P_{m,j+1} \exp\{-[\Gamma g_{m,j}(N_j) - \alpha_{int}]z\} dz = \frac{\exp\{[\Gamma g_{m,j}(N_j) - \alpha_{int}]\Delta L\} - 1}{[\Gamma g_{m,j}(N_j) - \alpha_{int}]\Delta L} P_{m,j+1} \quad (4)$$

$$\overline{P_{l,j}} = \frac{1}{\Delta L} \int_{(j-1)\Delta L}^{j\Delta L} P_{l,j-1} \exp\{[\Gamma g_{l,j}(N_j) - \alpha_{int}]z\} dz = \frac{\exp\{[\Gamma g_{l,j}(N_j) - \alpha_{int}]\Delta L\} - 1}{[\Gamma g_{l,j}(N_j) - \alpha_{int}]\Delta L} P_{l,j-1} \quad (5)$$

where  $\Delta L$  denotes the length of each SOA section,  $P_{m,j+1}$  and  $P_{l,j-1}$  are the modulation power output from the  $(j+1)$ th section and mode-locked power output from the  $(j-1)$ th section, respectively.  $g_{m,j}$  and  $g_{l,j}$  represent the asymmetric gain of the modulation and mode-locked signal, respectively, and are calculated by

$$g_{m,j} = \frac{a_1(N_j - N_0) - a_2(\lambda_m - \lambda_N)^2 + a_3(\lambda_m - \lambda_N)^3}{1 + \varepsilon(P_{m,j} + P_{l,j})} \quad (6)$$

$$g_{l,j} = \frac{a_1(N_j - N_0) - a_2(\lambda_l - \lambda_N)^2 + a_3(\lambda_l - \lambda_N)^3}{1 + \varepsilon(P_{l,j} + P_{m,j})} \quad (7)$$

where  $a_j$  is the differential gain coefficient,  $\lambda_m$  and  $\lambda_l$  are the central wavelength of the modulation and mode-locked signal, respectively,  $a_2$  and  $a_3$  are empirically determined constants that characterize the width and asymmetry of the gain profile, respectively,  $\varepsilon$  is the gain compression factor which is phenomenologically introduced to describe the effects of the carrier heating and spectral hole burning,  $N_0$  is the transparency carrier density,  $\lambda_N = \lambda_0 - a_4 (N_j - N_0)$  represents the corresponding peak gain wavelength with  $\lambda_0$  being the peak gain wavelength at transparency and  $a_4$

denoting the empirical constant that shows the shift of the gain peak.

Based on Eqs. (1) ~ (7) and using the fourth-fifth-order Runge-Kutta method, for a given input pulse passing through the modulation SOA, the temporal shape of output pulse can be simulated numerically. The procedure of the pulse amplification in the gain SOA can also be simulated with the similar method.

### 3. Results and discussion

The modulated optical signal output from the gain-switch DFBLD is assumed to be sinusoidal-wave with modulation frequency  $f_m = 2.5$  GHz. In this paper, we have assumed that the condition of harmonic mode locking and each-order rational harmonic mode locking are satisfied, and the other parameters used in the calculation are:  $\Gamma = 0.3$ ,  $L = 5 \times 10^{-4}$  m,  $\varepsilon = 0.2$  W<sup>-1</sup>,  $N_0 = 1.5 \times 10^{24}$  m<sup>-3</sup>,  $\lambda_0 = 1605$  nm,  $\lambda_s = 1550$  nm,  $\lambda_m = 1555$  nm,  $A = 2.5 \times 10^8$  s<sup>-1</sup>,  $B = 1 \times 10^{-17}$  m<sup>3</sup>s<sup>-1</sup>,  $C = 9.4 \times 10^{-41}$  m<sup>6</sup>s<sup>-1</sup>,  $a_1 = 2.5 \times 10^{-20}$  m<sup>2</sup>,  $a_2 = 7.4 \times 10^{19}$  m<sup>-3</sup>,  $a_3 = 3.155 \times 10^{25}$  m<sup>-4</sup>,  $a_4 = 3 \times 10^{-32}$  m<sup>4</sup>,  $\alpha_{int} = 2 \times 10^3$  m<sup>-1</sup>,  $A_{cross} = 4 \times 10^{-11}$  m<sup>2</sup>. Considering that the mode-locked signal pulse is generated from the spontaneous emission in the SOA, the initiated signal is assumed to be of very low power and independent on the time. At first, the initiated signal is modulated based on the cross-gain modulation when it passes through the modulation SOA and is amplified synchronously, then is gain-compensated by the gain SOA, after being attenuated by the OC, finally injects into the modulation SOA. Repeating continuously above process in the calculations, once the self-reproduction is satisfied, the stable mode-locked pulse can be specified.

#### 3.1 Harmonic mode locking

The optical signal (dot curve) output from the sinusoidal-wave-modulation DFBLD and the mode-locked pulse shape (solid curve) are shown in Fig. 2, where the bias currents of the modulation SOA and the gain SOA are 147 mA and 70 mA, respectively. From the diagram, it can be seen that, the mode-locked pulse is very narrow (the pulse width is less than 5 ps). The reason is that, in the high-current-biased modulation SOA, a backward injection can also induce a strong gain-depletion (or loss) modulation, which can suppress the temporal shift and the pedestal amplitude of mode-locked pulse. Moreover, a narrow temporal range of the net gain can be obtained in a relatively low bias current of the gain SOA.

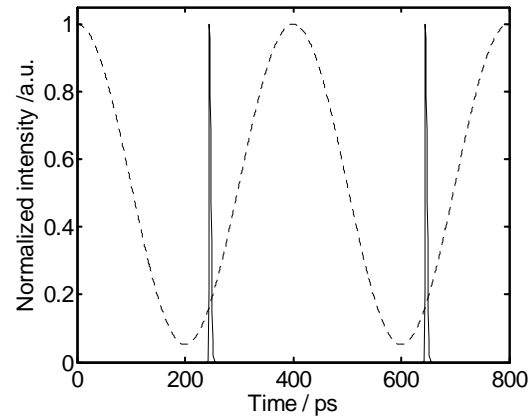


Fig. 2. Optical signal (dot curve) output from the sinusoidal-wave-modulation DFBLD and the mode-locked pulse shape (solid curve).

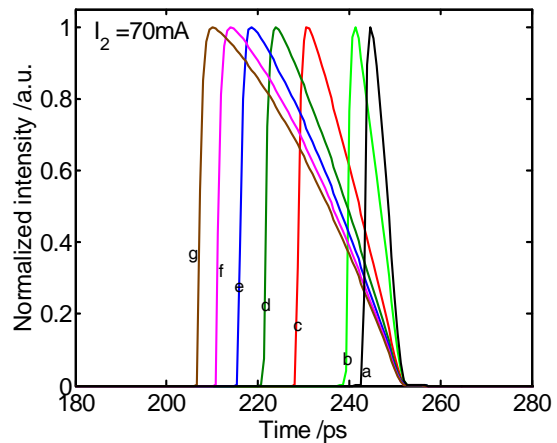


Fig. 3. Normalized wave shape out from the mode-locked SOA fiber laser with different biased conditions of the modulation SOA.

Normalized wave shapes output from the mode-locked SOA fiber laser with different biased condition of the modulation SOA are shown in Fig. 3, where the bias current of the gain SOA is 70 mA, and the bias current of the modulation SOA is 174 mA (curve a), 175 mA (curve b), 180 mA (curve c), 185 mA (curve d), 190 mA (curve e), 195 mA (curve f), and 200 mA (curve g), respectively. As we can see, when the bias current of the modulation SOA is 174 mA, the output pulse is the narrowest and with a symmetrical temporal shape. With the increase of the bias current of the modulation SOA, pulse width is gradually widened. Moreover, pulse leading edge becomes steep and trailing edge becomes slow, which is caused by saturated gain in SOA.

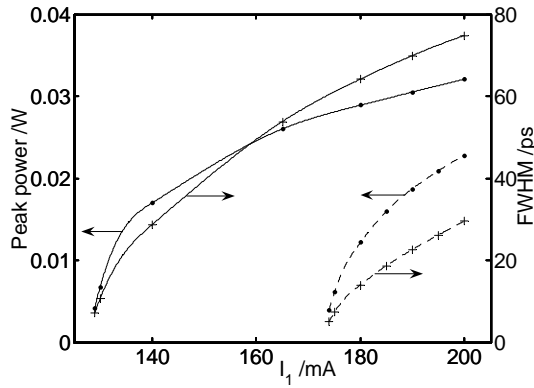


Fig. 4. The peak-power and pulse-width of the mode-locked pulse versus the bias current of the modulation SOA, where the solid curve is for the bias current of the gain SOA  $I_2 = 80$  mA and the dot curve is for  $I_2 = 70$  mA.

Fig. 4 shows the peak power and pulse width of mode-locked pulse versus the bias current of the modulation SOA, where the solid curve is for the bias current of the gain SOA  $I_2 = 80$  mA and the dash-dot curve is for  $I_2 = 70$  mA. From this diagram, it can be seen that, with the increase of the bias current of the modulation SOA, the peak power is enhanced and the pulse width is widened, which is easy to understand. Because part of the carriers is depleted by the modulation signal and only the residual carriers are used to amplify the mode-locked pulse, with the increase of the bias current of the modulation SOA, the residual carriers will increase, which results in the increase of the peak power. Meantime, the time range within which the small signal gain is more than cavity loss will be added, which results in the pulse-width widen. If the bias current of the modulation SOA is maintained a constant, different peak powers and pulse widths can be obtained through adjusting the bias current of the gain SOA. Through calculations, it can be concluded that the mode-locked pulse with large peak power and narrow width can be obtained when the bias current of the modulation SOA is biased high enough and the current of the gain SOA is biased relatively low to realize that the net gain of small signal is larger than zero. It should be pointed out that, with the increase of the modulation frequency, the peak power of mode-locked pulse will decrease because the gains of the SOAs cannot be fully recovered, moreover, the width of mode-locked pulse will also decrease because of the net gain time range decrease.

### 3.2 Rational harmonic mode locking

Using the experiment setup in Fig. 1, rational harmonic mode locking also can be realized by adjusting the length of the ring cavity or changing the modulation frequency. However, pulse-amplitude equalization cannot be obtained only by adjusting the bias current of SOAs, which may be also related to the intensity of the

modulation signal, therefore, an EDFA is added to the experiment setup in Fig. 1 to enhance the optical-signal power emitted by the gain-switch DFBLD.

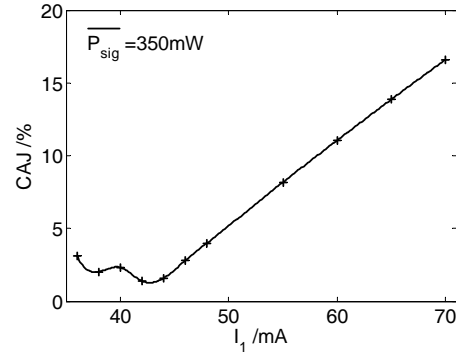


Fig. 5. CAJ of the second-order RHML pulses versus the bias current of the modulation SOA.

The quality of pulse-amplitude equilibrium can be measured by the clock amplitude jitter (CAJ) [12]

$$CAJ = \frac{\sigma}{M} \times 100(\%) \quad (1)$$

where  $\sigma$  is the standard deviation and  $M$  is the mean of the intensity histogram at the peak of pulses. Normally, CAJ is related to the system parameters. Fig. 5 shows CAJ of the second-order RHML pulses versus the bias current of the modulation SOA, where the average power of the modulation optical signal is 350 mW and the bias current of the gain SOA are 95 mA, respectively. From this diagram, it can be seen that, the effect of the bias current of the modulation SOA on CAJ of RHML pulses is great. There exists a minimum of CAJ less than 1.38% (which denote the pulses are quite even), when the bias current of the modulation SOA is about 42 mA. However, with the increase of the bias current of modulation SOA, CAJ rapidly increases.

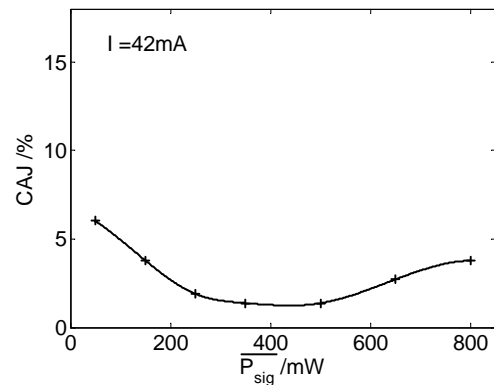


Fig. 6. CAJ of the second-order RHML pulses versus the modulation-optical power.

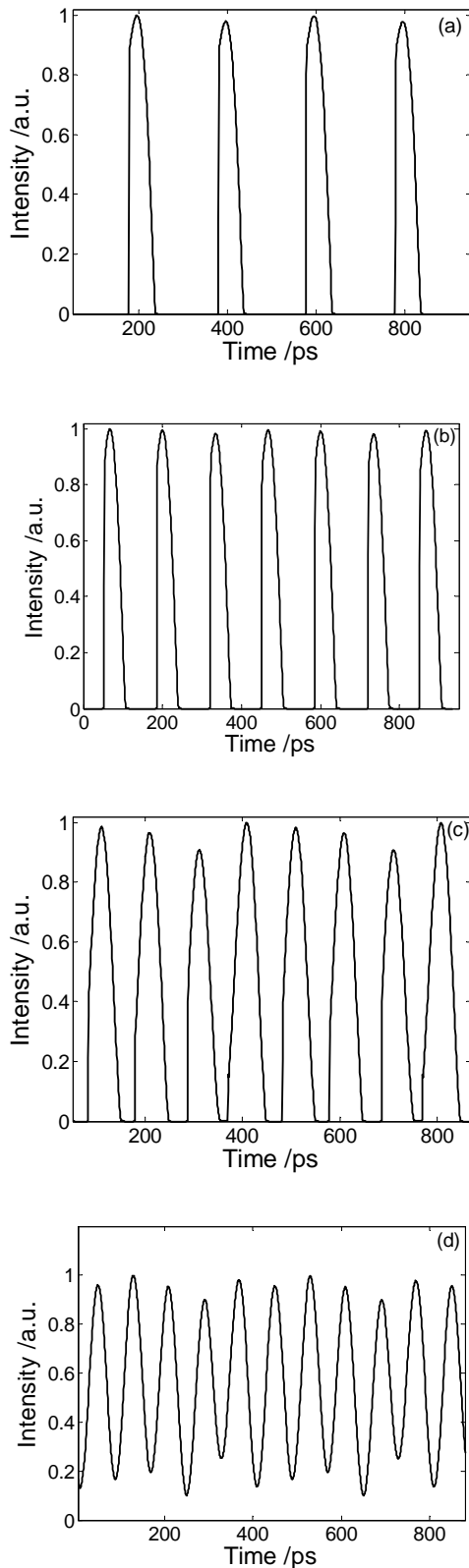


Fig. 7. Wave shapes of the 2~5th order RHML pulse.

Fig. 6 shows  $CAJ$  of the second-order RHML pulses versus the modulation-optical power, where the bias current of the modulation SOA and the gain SOA are 42mA and 95mA, respectively. From this diagram, it can be seen that, with the increase of the average-optical power,  $CAJ$  of the second-order RHML pulses decreases at first, after passing through a minimum where the average-optical power is 350 mW, then increases. According to rational harmonic mode locking mechanism, the modulation frequency  $f_m$  is slightly detuned from the harmonic mode-locked condition by  $f_c/p$ , which means that pulse after running a circle will have a time interval of  $T_m/p$  ( $T_m$  is modulation period, and  $T_m = 1/f_m$ ) with initial pulse, and after passing through  $p$  times circulation, a full modulation is accomplished. Different from harmonic mode locking, a high-power-injected modulation is necessary. On the contrary, if the injected-modulation-single intensity is too high, carriers will be depleted overmuch, resulting in the decline of the modulation SOA gain, which makes  $CAJ$  increase, too.

To realize pulse-amplitude equilibrium of rational harmonic mode locking, the bias current of the modulation SOA and the injected-modulation-optical power should be synchronously adjusted. Fig. 7(a) ~ (d) shows wave shape of the 2~5th order RHML pulse after optimizing parameters, respectively. From this diagram, it can be seen that, amplitude of the 2~5th order RHML pulse are comparatively even, and if the system parameters are carefully adjusted, the quality of pulse-amplitude equilibrium will be more improved. However, when rational harmonic mode locking is over 4 orders, extinction-ratio of the output pulses begins to decline, which is caused by relatively slow carrier-resuming time.

#### 4. Conclusions

It has been numerically proved that the quality of harmonic mode-locked pulse can be improved when the modulation SOA is in high-biased condition whereas the gain SOA is in low-biased condition functions as gain compensator. However, to realize pulse-amplitude equalization of rational harmonic mode locking, the modulation SOA should bias in low-biased condition whereas the gain SOA should bias high-biased condition. Besides, an EDFA should be added to enhance the pulse power output from DFB-LD.

#### Acknowledgements

The authors acknowledge the support from the Key Project of the Ministry of Education of the People's Republic of China and the Commission of Science and the Natural Science Foundation of Chongqing City of the People's Republic of China under Grant CSTC-2005BB3099.

## References

- [1] D. J. Jones, H. A. Haus, E. P. Ippen, *Opt. Lett.* **21**(22), 1818 (1996).
- [2] D. Pudo, L. R. Chen, D. Giannone, L. Zhang, I. Bennion, *IEEE Photon. Technol. Lett.* **14**(2), 143 (2002).
- [3] S. P. Li, K. T. Chan, *Appl. Phys. Lett.* **72**(16), 1954 (1998).
- [4] J. M. Roth, K. Dreyer, B. C. Collings, W. H. Knox, K. Bergman, *IEEE Photon. Technol. Lett.* **14** (7), 917 (2002).
- [5] C. Wu, N. K. Dutta, *IEEE J. Quantum Electron.* **36**(2), 145 (2000).
- [6] P. Can, M. Y. Yao, J. F. Zhang, H. M. Zhang, Q. F. Xu, Y. Z. Gao, *Opt. Commun.* **209**(4-6), 181 (2002).
- [7] D. M. Patrick, *Electron. Lett.* **30**(1), 43 (1994).
- [8] T. Papakyriakopoulos, K. Vlachos, A. Hatziefremidis, H. Avramopoulos, *Opt. Lett.* **24**(17), 1209 (1999).
- [9] G. R. Lin, Y. S. Liao, G. Q. Xia, *Opt. Express* **12**(10), 2017 (2004).
- [10] Wenyan Yang, Zhengmao Wu, Guangqiong Xia, *Opt. Commun.* **250**(4-6), 384 (2005).
- [11] M. Y. Jeon, H. K. Lee, J. T. Ahn, D. S. Lim, H. Y. Kim, K. H. Kim, *Electron. Lett.* **34**(2), 182 (1998).
- [12] H. J. Lee, K. Kim, H. G. Kim, *Opt. Commun.* **160** (1-3), 51 (1999).
- [13] K. K. Gupta, N. Onodera, M. Hyodo, *Electron. Lett.* **37**(15), 948 (2001).
- [14] Fei Wang, Guangqiong Xia, Zhengmao Wu, *Opt. Commun.* **257**(2), 334 (2006).

---

\*Corresponding author: zmwu@swu.edu.cn